J Membrane Biol (2007) 215:1–13
DOI 10.1007/s00232-007-9000-9

TOPICAL REVIEW

Role of Calcium in Volume-Activated Chloride Currents in a Mouse Cholangiocyte Cell Line

Biyi Chen · Grant Nicol · Won Kyoo Cho

Received: 30 August 2006 / Accepted: 6 January 2007 / Published online: 5 May 2007

Abstract Volume-activated Cl^- channels (VACCs) play vital roles in many cells including cholangiocytes. Previously, we characterized the VACCs in mouse cholangiocytes. Since calcium plays an important role in VACC regulation in many cells, we have studied the effect of calcium modulation on the regulatory volume decrease (RVD) and VACC currents in mouse bile duct cells (MBDCs). Cell volume measurements were assessed by a Coulter counter with cell sizer, and conventional whole-cell patch-clamp techniques were used to study the role of calcium on RVD and VACC currents. Cell volume study indicated that MBDCs exhibited RVD, which was inhibited by 5-nitro-2′-(3-phenylpropylamino)-benzoate (NPPB), 4,4′-diisothiocyanostilbene-2,2′-disulfonate (DIDS) and 1,2-bis (*o*-aminophenoxy)ethane-*N,N,N′,N′*-tetraacetic acid tetraacetoxymethyl ester (BAPTA-AM) but not by removal of extracellular calcium. During hypotonic challenge, MBDCs exhibited an outwardly rectified current, which was significantly inhibited by administration of classical chloride channel inhibitors such as NPPB and tamoxifen. Chelation of the intracellular calcium with BAPTA-AM or removal of extracellular calcium and calcium channel blocker had no significant effect on VACC currents during hypotonic challenge. In addition to VACC, MBDC had a calcium-activated chloride channel, which was inhibited by NPPB. The present study is the first to systemically study the role of calcium on the VACC and RVD in mouse cholangiocytes and demonstrates that a certain level of intracellular calcium is necessary for RVD but the activation of VACC during RVD does not require calcium. These findings suggest that calcium does not have a direct regulatory role on VACC but has a permissive role on RVD in cholangiocytes.

Keywords Bile duct cell · Cell volume · Mouse cholangiocyte · Volume-activated chloride channel · Ion channel · Calcium · Patch clamping · Regulatory volume decrease

B. Chen · W. K. Cho
Division of Gastroenterology/Hepatology, Department of Medicine, Indiana University School of Medicine and The Richard L. Roudebush Veterans Affairs Medical Center, 1481 W. 10th Street, Indianapolis, IN 46202, USA

G. Nicol
Department of Pharmacology and Toxicology, Indiana University School of Medicine, 635 Barnhill Drive, RM A402, Indianapolis, IN 46202, USA

W. K. Cho (✉)
Roudebush VA Medical Center, Division of GI/Hepatology (111G), Indiana University School of Medicine, 1481 W. 10th Street, Indianapolis, IN 46202, USA
e-mail: wkcho@iupui.edu

Introduction

Osmoregulation is an essential cellular function necessary to maintain constant cell volume and regulate internal composition in response to changes in the osmolarity of the extracellular solution (Lang et al. 1998; Sardini et al. 2003). When many different types of cells are swollen after exposure to hypotonic solution, they undergo regulatory volume decrease (RVD), which involves the extrusion of intracellular K^+ and Cl^- ions to return toward their original cell volumes (Hoffmann and Simonsen 1989; Kirk 1997; Nilius and Droogmans 2003; Sardini et al. 2003; Cho 2002). The volume-activated chloride channel (VACC) mediates the chloride conductance to extrude Cl^- ions during RVD, in conjunction with K^+ channels (Nilius and Droogmans 2003; Nilius et al. 1997; Cho 2002).

Under physiological conditions, bile duct cells or cholangiocytes are exposed to various osmotic stresses from uptake of inorganic and organic solutes, as well as modification and secretion of bile (Graf and Haussinger 1996; Lira et al. 1992). A study in the Mz-ChA-1 human cholangiocarcinoma cell line (Roman, Wang and Fitz 1996) as well as our study in primary bile duct cell clusters from normal mouse livers (Cho 2002) have indicated that cholangiocytes can also regulate their cell volumes back toward baseline when exposed to hypotonic solution by increasing K^+ and Cl^- conductances. In addition, these studies have shown that the chloride conductance during RVD in mouse cholangiocytes is mediated by a VACC; characterized by an outwardly rectified chloride current, with time-dependent inactivation at depolarizing potentials; and inhibited by classic chloride blockers, such as 5-nitro-2′-(3-phenylpropylamino)-benzoate (NPPB), glybenclamide, 4,4′-diisothiocyanostilbene-2,2′-disulfonate (DIDS) and tamoxifen (Roman et al. 1996; Chen, Nicol and Cho 2004).

In some cells, an increase in intracellular calcium levels is observed during RVD and is considered important for the activation of VACC (Diaz et al. 1993; Basavappa et al. 1995; Lemonnier et al. 2002). However, other cells do not show such increase in intracellular Ca^{2+} levels during RVD, and their VACC was not affected by extracellular calcium and calcium channel antagonists (Fatherazi et al. 1994; Best, Sheader and Brown 1996; Wu et al. 1996; Leaney, March and Brown 1997; Pedersen et al. 1998, Von Weikersthal, Barrand and Hladky 1999). In Mz-ChA-1 human cholangiocarcinoma cells, chelation of cytosolic Ca^{2+} inhibited swelling-induced isotope efflux, prevented activation of macroscopic K^+ and Cl^- currents and blocked volume recovery (Roman et al. 1996). However, the isotope efflux study is not specific for VACC, and it is possible that the observed inhibitory effects of chelating calcium on chloride efflux may be due to its effect on other channels such as the calcium-activated chloride channel. In spite of the potential importance of calcium in RVD and VACC activation, the effect of calcium on VACC in cholangiocytes is not well studied. Thus, in the present study, the role of calcium on RVD was examined using cell volume measurements with a cell sizer as well as on VACC using whole-cell patch-clamp techniques in a normal mouse bile duct cell (MBDC) line, conditionally immortalized by simian vacuolating virus 40 (SV40) (Paradis et al. 1995).

Materials and Methods

Materials

Bovine serum albumin, penicillin/streptomycin, ethylene glycol-bis(b-aminoethyl ether)-*N,N′,N*-tetraacetic acid (EGTA), 4-(2-hydroxy-ethyl)-1-piperazine ethanesulfonic acid (HEPES), D$^+$-glucose, dimethyl sulfoxide, tamoxifen, sodium gluconate, L-thyroxine, prostaglandin E_1 and hydrocortisone were purchased from Sigma (St. Louis, MO). Epidermal growth factor, insulin, transferrin, selenium, Matrigel and dispase were purchased from Collaborative Biomedical (Bedford, MA); and mouse recombinant interferon-γ (IFN-γ) was purchased from Boehringer-Mannheim (Indianapolis, IN). Minimal essential medium (MEM)/F12 with glutamine, nonessential amino acid solution, fetal calf serum and trypsin were from GIBCO (Grand Island, NY). NPPB and ionomycin were from Calbiochem (San Diego, CA). The SV40-transformed, conditionally immortalized MBDC line was a generous gift from Dr. K. Paradis (Montreal, Canada).

Solutions

Isotonic and hypotonic solution compositions were as described previously (Chen et al. 2004) and are briefly outlined below. The actual osmolarities of the solutions were determined by the Vapor Pressure Osmometer 5500 (Wescor, Logan, UT).

Bathing Solution

Isotonic bathing solution contained (in mM) NaCl 100, sucrose 80, KCl 4, $CaCl_2$ 1, $MgCl_2$ 2, KH_2PO_4 1, HEPES 10 and glucose 5. Osmolarity was 301 mOsm (measured by vapor pressure osmometer), with pH adjusted to 7.4 with NaOH.

Hypotonic bathing solution contained (in mM) (Nilius et al. 1997; Singh, Venglarik and Bridges 1995) NaCl 100, KCl 4, $CaCl_2$ 1, $MgCl_2$ 2, KH_2PO4 1, HEPES 10 and glucose 5. Osmolarity was 223 mOsm, with pH adjusted to 7.4 with NaOH.

Calcium-free hypotonic bathing solution contained (in mM) (Nilius et al. 1997; Singh et al. 1995) NaCl 100, KCl 4, $MgCl_2$ 2, KH_2PO4 1, HEPES 10, EGTA 1 and glucose 5. Osmolarity was 221 mOsm, with pH adjusted to 7.4 with NaOH.

Pipette Solution

Standard pipette solution contained (in mM) CsCl 100, sucrose 60, NaCl 10, $MgCl_2$ 1, $CaCl_2$ 0.1, HEPES 10, EGTA 1, MgATP 5 and Na_2GTP 0.1. Osmolarity was 281 mOsm, with pH adjusted to 7.3 with KOH.

Ca-free pipette solution contained (in mM) CsCl 100, sucrose 60, NaCl 10, $MgCl_2$ 1, HEPES 10, EGTA 1, MgATP 5 and Na_2GTP 0.1. Osmolarity was 281 mOsm, with pH adjusted to 7.3 with KOH.

Cell Culture

The mouse cell line used in this study is conditionally immortalized by SV40 and was shown to be stable, well-differentiated and polarized and to express cytokeratin 19 (Paradis et al. 1995). It can also form duct-like structures and proliferate in response to epithermal growth factor, interleukin 1α and tumor necrosis factor α (Paradis et al. 1995). These cells were grown in monolayer culture in MBDC medium as previously described (Paradis et al. 1995). The cells were grown on Matrigel-coated flasks at 33°C in humidified atmosphere of 5% CO_2, and medium was replaced every 3–4 days. The cells were passaged every 14 days after digestion with 0.04% dispase and 0.01% trypsin.

Cell Volume Measurement

Mean cell diameter (MCD) was measured in cell suspensions at 25°C using electronic cell sizing by the Coulter Multisizer 3 and Multisizer software (version 3.51; Beckman Coulter, Fullerton, CA) with an aperture tube diameter of 100 μm; mean cell volume (MCV) was calculated utilizing the formula $4/3\pi r^3$. The instrument was calibrated with polystyrene beads of known dimensions (Beckman Coulter). Approximately 8 million cells grown on polystyrene flasks (Costar, Cambridge, MA) were harvested with 0.05% trypsin, suspended in Ca^{2+}- and Mg^{2+}-free phosphate-buffered saline and cell culture medium (to inactivate trypsin), centrifuged for 1 min at 1,000 revolutions/min (~2,000 × *g*), resuspended in 4 ml of isotonic solution and incubated with gentle agitation for 45 min at 37°C. Aliquots (500 μl) of isotonic cell suspension were then added to 100 ml of either isotonic or hypotonic (27% decrease in NaCl) solutions at time 0 s. Measurements were obtained from about 10,000 cells at -5 min (basal isotonic cell volume) and at every 1 min after exposure to control or experimental solutions. To chelate $[Ca^{2+}]_i$, 1,2-bis(*o*-aminophenoxy)ethane-*N,N,N′,N′*-tetraacetic acid tetra-acetoxymethyl ester (BAPTA-AM, 30 μM) was added to isotonic solution during the 5-min incubation before hypotonic stress. Changes in size over time are expressed as relative volume percent changes by normalizing volume to the basal volume during the preincubation period, and control and experimental values are presented as percent ± standard deviation (SD) for statistical comparison of various conditions.

Patch Clamp

For patch-clamp experiments, the cells were plated on Matrigel-coated rectangular glass coverslips (2–4 mm) and cultured at 37°C. After the cells were cultured 7–10 days, they were moved to a specimen chamber on an inverted Nikon (Tokyo, Japan) microscope and perfused with bath solution at room temperature (23–25°C). Whole-cell currents were measured in the conventional configuration of the patch-clamp technique, using an Axopatch-1D amplifier (Axon Instruments, Foster City, CA). Pipettes were prepared (resistance 4–5 MΩ) from borosilicate capillary tubes (1.0 mm outer diameter, 0.5 mm inner diameter; Sutter Instruments, Novato, CA) using a P-87 Flaming/Brown micropipette puller (Sutter Instruments, San Rafael, CA). To specifically measure chloride currents, potassium in the pipette solution was completely replaced with cesium. The junction potentials were determined by immersing the pipette into the bath filled with pipette solution, zeroing the voltage reading (Li et al. 2000). After forming a gigaseal, the fast-compensation system of the amplifier was used to compensate for the intrinsic input capacitance of the head-stage and the pipette. The whole-cell recording configuration was usually established by applying brief suction to disrupt the patch membrane. The membrane capacitance and series resistance were compensated (80%) to minimize the capacitive transient and to improve the dynamic response. The reference electrode was Ag/AgCl. The current-voltage relationships between –120 and 130 m*V* were measured by voltage steps in 10-m*V* increments, 200 ms, 1 Hz and holding potential 0 m*V* in isotonic and hypotonic bathing solutions as indicated. The current was acquired and analyzed using pClamp software (Axon Instruments). The chloride current amplitude was measured at the end of the 200-ms pulse.

Data And Statistical Analysis

All measurement data are expressed as mean ± SD. Using Excel computer software (Microsoft Software, San Diego, CA), Student's paired and unpaired *t*-tests were performed for statistical data analysis.

Results

Study of Cell Volume Changes

To characterize the RVD of MBDCs, serial changes in MBDC volumes were examined after exposure to hypotonic solution using Coulter counter methods. Under isotonic conditions, the MCD of mouse cholangiocytes was 12.68 ± 1.18 μm, corresponding to an MCV of 1,067.5 ± 327 μm^3 (n = 16). Basal isotonic volume did not significantly change during incubation in isotonic solution. However, as shown in Figure 1A, exposure of MBDCs to hypotonic buffer (27% decrease in NaCl)

caused a rapid initial increase in MCV within 5 min to a relative cell volume of 1.16 ± 0.04 (n = 5, $P < 0.001$ *vs.* basal cell volume). Swelling was followed by an RVD that showed a gradual decrease in MCV to a relative volume of 1.09 ± 0.01 by 10 min and returned to basal cell volume at 30 min to a relative volume of 1.00 ± 0.02.

To confirm involvement of chloride channels in the observed RVD of MBDCs, we studied the effect of chloride channel inhibitors on cell volume changes. As shown in Figure 1B, coadministration of NPPB (40 μM) with hypotonic solution inhibited the RVD, and the relative MCV after 30 min of hypotonic challenge was 1.06 ± 0.03, which was statistically significant ($P < 0.05$) compared to the RVD seen with control MBDCs (1.00 ± 0.02). In addition, as shown in Figure 1C, another chloride channel blocker, DIDS (250 μM), significantly ($P < 0.05$) inhibited the RVD of MBDCs, and the relative MCV of DIDS-treated MBDCs after hypotonic challenge was 1.10 ± 0.03 compared to 1.00 ± 0.01 in untreated controls. These results are consistent with our previous findings in a primary MBDC cluster volume study (Cho 2002) as well as an electrophysiolgical study in MBDCs (Chen et al. 2004), confirming the involvement of VACCs in the RVD of mouse cholangiocytes.

To study the role of extracellular calcium on the RVD, cell volume changes were examined after exposing MBDCs to calcium-free hypotonic solution. As shown in Figure 1D, removal of calcium from the hypotonic solution had no significant effect on RVD, indicating that extracellular calcium had no significant role in the RVD of cholangiocytes. To study the role of intracellular calcium, BAPTA-AM (30 μM) was added to hypotonic solution and the changes in cell volume with hypotonic challenge were examined. As shown in Figure 1E, administration of BAPTA-AM significantly ($P < 0.001$) inhibited the RVD of MBDCs compared to control, and the relative MCV at 30 min was 1.13 ± 0.03.

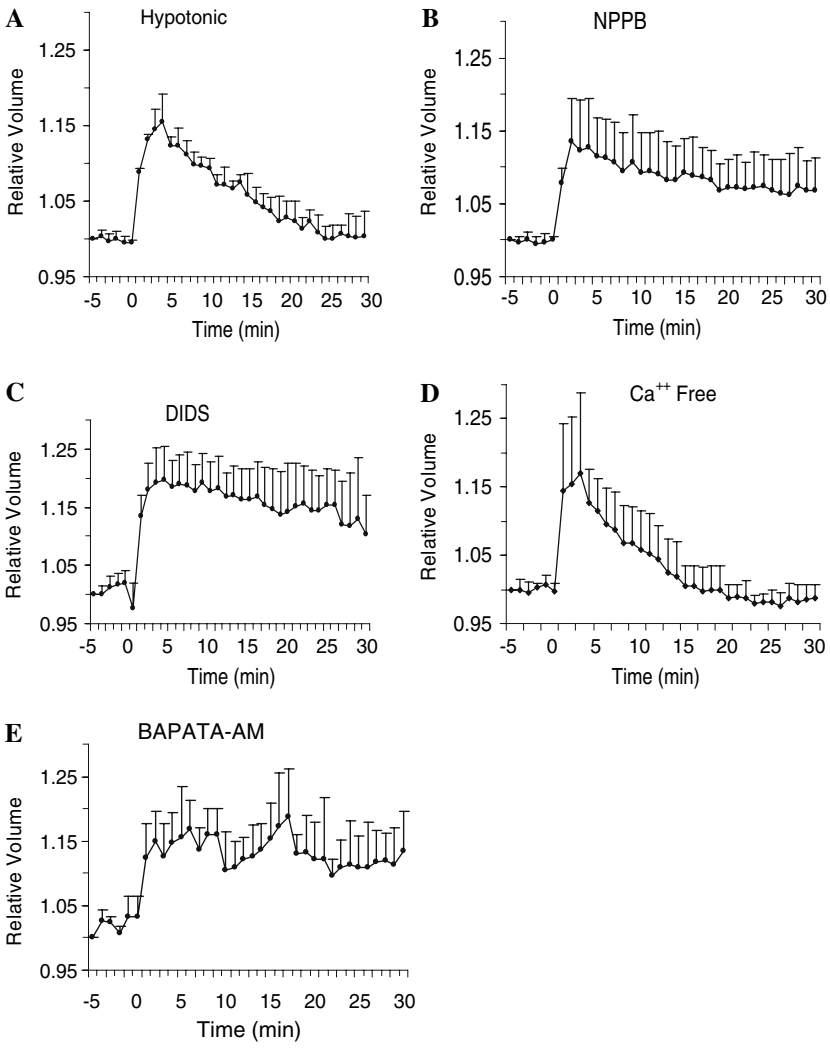

Fig. 1 Effect of NPPB, DIDS, Ca^{2+} and BAPTA-AM on RVD of MBDCs. The effects of various modified hypotonic solutions on RVD of MBDCs were examined using a Coulter counter: (*A*) hypotonic, (*B*) NPPB 40 μM, (*C*) DIDS 250 μM, (*D*) calcium-free, (*E*) BAPTA-AM 30 μM; n = 5–6, mean ± SD

Electrophysiologic Study

Study of VACCs

To further characterize the VACC, we performed detailed patch-clamping studies using the techniques reported previously (Chen et al. 2004). To study the effect of hypotonic challenge on the chloride currents in MBDCs, the currents were measured in isotonic solution, then again after switching the bathing solution to hypotonic solution. Figure 2A shows typical membrane current recordings and current-voltage (*I-V*) curves, and Figure 2B shows the time course of the membrane current. As shown in Figure 2A, the voltage steps elicited baseline currents that were small, outwardly rectified currents with a reversal potential of –2.5 ± 9.57 m*V* (n = 4 *vs.* calculated value of –1 m*V*). When MBDCs were exposed to hypotonic solution, significantly (n = 4, $P < 0.01$) larger currents (3.52 ± 2.27 nA in hypotonic solution *vs.* 0.56 ± 0.32 nA in isotonic solution at 120 m*V* depolarization) were observed within 3–5 min, reaching a peak within 5–10 min (Fig. 2B) and had the same outwardly rectified configuration with a slight time-dependent inactivation (Fig. 2A) as with the basal currents. The amplitude of the initial currents recorded at +120 m*V* was about 2.8 times that of the currents recorded at –120 m*V*, and their reversal potential was not shifted significantly (0.5 ± 6.45 m*V*, n = 4, *vs.* calculated expected value of 1 m*V*) from baseline of 0 m*V*. When the cell was reexposed to isotonic solution, these volume-activated currents returned back to baseline levels. These results are summarized in Figure 2C, which shows that hypotonic challenge significantly stimulated membrane currents in MBDCs, and these volume-activated currents returned to basal level when the cells were reexposed to isotonic solution. Previously, we extensively characterized this volume-activated current as a VACC (Chen et al. 2004).

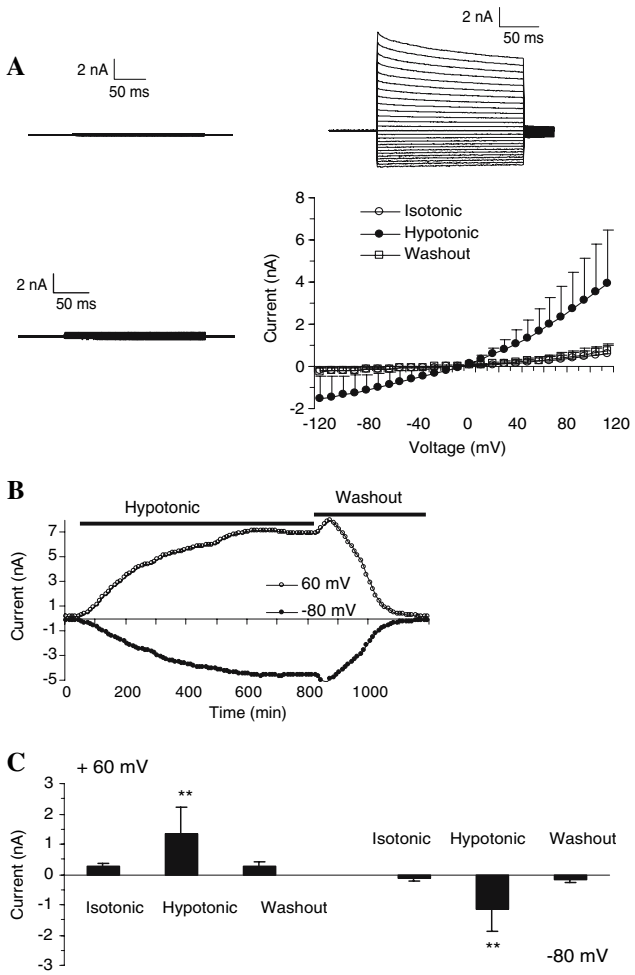

Fig. 2 Volume-activated chloride current in MBDCs. Whole-cell currents were measured using isotonic and hypotonic standard bathing solutions and standard cesium pipette solution. (*A*) Representative traces and *I-V* curves of the volume-activated chloride currents. Currents were measured using voltage steps from –120 to 130 m*V* in 10-m*V* increments at 200 ms, 1 Hz from holding potential 0 m*V*. (*B*) Time course of the volume-activated chloride current, holding potential 0 m*V*, voltage step 60 and –80 m*V* at 200 ms and 0.1 Hz. (*C*) Summary of volume-activated chloride currents, n = 6, mean ± SD, $^{**}P < 0.01$

Role of Extracellular Calcium on Volume-Activated Chloride Current

To determine the role of extracellular calcium on the VACC during hypotonic challenge, the effect of removing calcium from the hypotonic solution on volume-activated currents was examined, as shown in Figure 3. Figure 3A shows the current tracings and *I-V* relationship, and Figure 3B shows the time course of the currents. Under basal conditions in isotonic solution, the voltage step protocol elicited a small current with a reversal potential near zero (2.1 ± 5.6 m*V*, n = 4, *vs.* calculated –1 m*V*). In addition, as with controls in normal hypotonic solution, these voltage steps induced a large increase in whole-cell current ($P <$ 0.01 *vs.* control isotonic) in calcium-free hypotonic solution, and the reversal potential also was not shifted significantly (1.0 ± 5.2 m*V* *vs.* calculated 1 m*V*). Again, when the cells were reexposed to isotonic solution, the currents returned to the basal level ($P < 0.01$ *vs.* hypotonic solution, $P > 0.05$ *vs.* control isotonic solution). Figure 3C shows the effect of removing extracellular calcium on the *I-V* curves of volume-activated chloride currents. The *I-V* curve was not shifted significantly ($P < 0.01$) when the cells were exposed to calcium-free hypotonic solution compared to normal hypotonic solution. Figure 3D is a summary of the effect of removing extracellular calcium on the volume-activated chloride currents, showing that the currents were not significantly affected by removal of extracellular

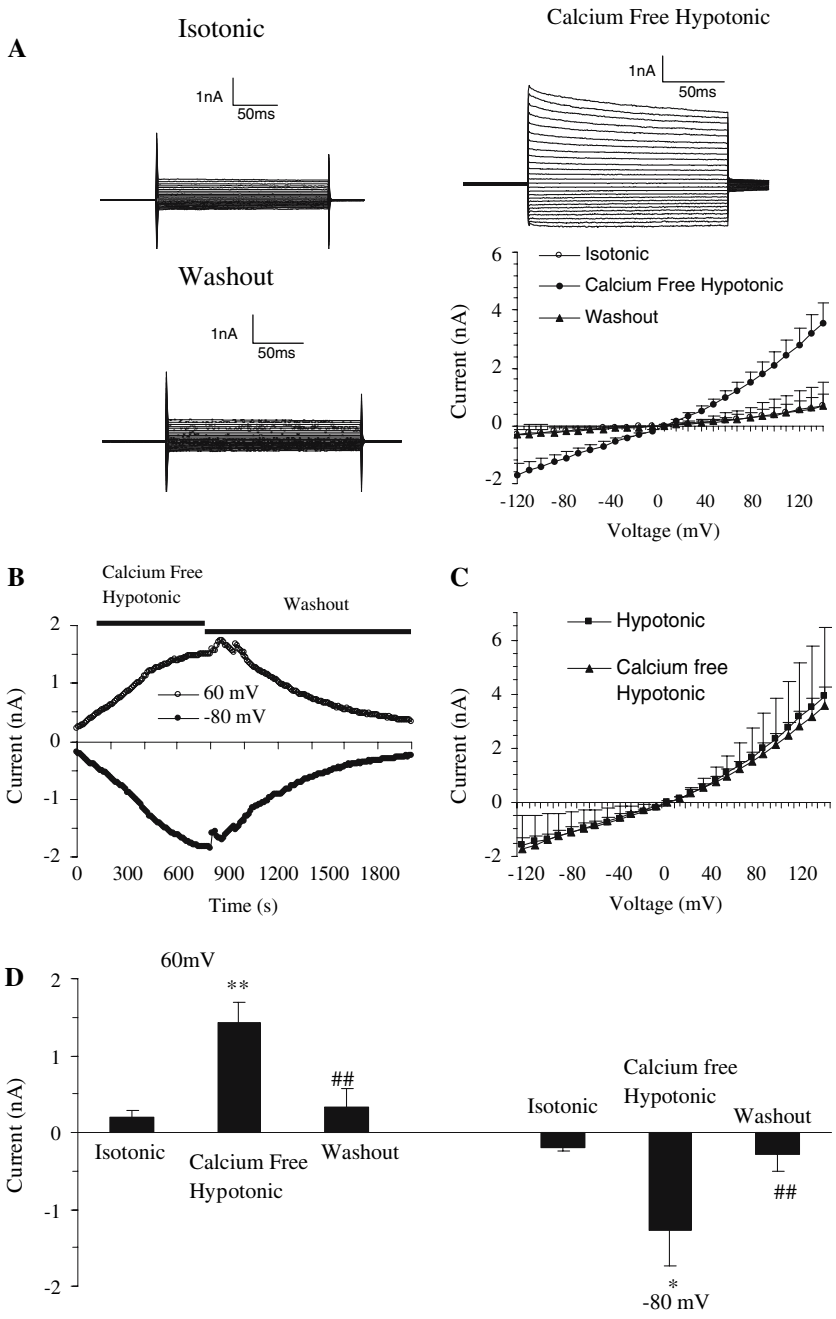

Fig. 3 Effect of extracellular calcium on volume-activated chloride current. (*A*) Representative traces and *I-V* curves of the volume-activated chloride current in calcium-free hypotonic bathing solution. Currents were measured using voltage steps from –120 to 130 m*V* in 10-m*V* increments, 200 ms, holding potential 0 m*V*. (*B*) Time course of the volume-activated chloride current in calcium-free hypotonic bathing solution and cesium pipette solution with holding potential – 0 m*V*, voltage from –120 to 130 m*V*, 200 ms, 0.1 Hz. (*C*) Comparison of *I-V* curves of volume-activated chloride currents in hypotonic and calcium free hypotonic solutions. (*D*) Summary of the effect of extracellular calcium on volume-activated chloride currents, mean ± SD, $n = 5$, $^{*}P < 0.05$, $^{**}P < 0.01$ vs Isotonic, $\#\#P < 0.01$ vs Calcium Free Hypotonic

calcium from the bathing solution and still could be activated during hypotonic challenge.

Role of Intracellular Calcium on Volume-Activated Chloride Current

To determine the role of intracellular calcium on volume-activated chloride currents during hypotonic challenge, the currents were measured with hypotonic solution containing BAPTA-AM (30 μM). As shown in Figure 4A, exposure of MBDCs to hypotonic solution containing BAPTA-AM also induced significantly ($P < 0.05$ *vs.* isotonic control) larger outwardly rectified currents. These large outwardly rectified currents also showed a slight time-dependent inactivation. The *I-V* curve (Fig. 4A) shows that large outwardly rectified currents were induced when switching the bathing solution from isotonic to hypotonic solution containing BAPTA-AM, while the reversal potential was not shifted significantly (0.4 ± 2.9 m*V*, $n = 5$, *vs.* calculated 6.8 m*V*). When the cells were reexposed to the isotonic solution, the currents returned to basal level ($P < 0.001$ *vs.* hypotonic). Figure 4B shows the time course of the volume-activated chloride current observed when MBDCs were exposed to hypotonic

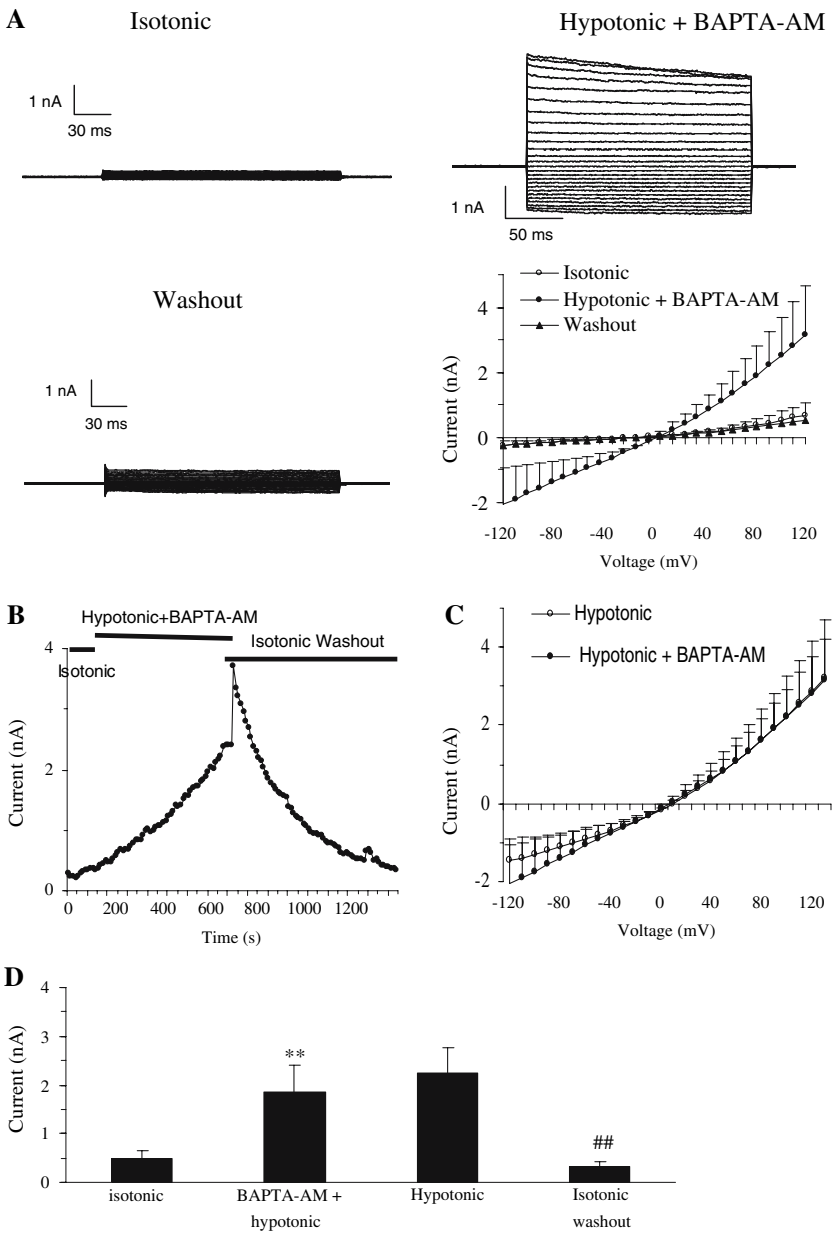

Fig. 4 Effect of BAPTA-AM on volume-activated chloride currents. (*A*) Representative traces and *I-V* curve. Currents were measured using voltage steps from –120 to 130 m*V* in 10-m*V* increments at 200 ms, 1 Hz from holding potential 0 m*V*. (*B*) Time course of volume-activated chloride currents in hypotonic and calcium-free hypotonic solutions, holding potential 0 m*V*, voltage step 60 and –80 m*V* at 200 ms, 0.1 Hz. (*C*) Comparison of *I-V* curves of volume-activated chloride currents in hypotonic and BAPTA-AM hypotonic solutions. (*D*) Summary of the effect of BAPTA-AM on volume-activated chloride currents, $n = 6$, mean ± SD, $^{**}P < 0.01$ vs Isotonic, $\#\#P < 0.01$ vs Hypotonic

solution containing BAPTA-AM. The depolarizing steps elicited a large outward current, reaching the maximum at 5–10 min, then the currents returned to basal level within 5–10 min after reexposing the cells to isotonic solution. As shown in Figure 4C, a chelation of intracellular calcium by BAPTA-AM had no significant effect on the *I-V* curves of volume-activated chloride currents compared to untreated controls. Figure 4D shows a summary of the effect of BAPTA-AM on volume-activated chloride currents induced at 60 m*V*. The currents increased approximately sixfold ($P < 0.01$) when the cells were exposed to hypotonic solution containing BAPTA-AM but were not significantly different from the VACC currents of untreated controls.

Effect of Verapamil on Volume-Activated Chloride Currents

To further study the role of the calcium channel on VACCs, the effect of a calcium channel blocker, verapamil (20 μM), on VACCs was examined (Fig. 5). When the MBDCs were exposed to hypotonic solution containing verapamil, the amplitude of the volume-activated chloride currents was not significantly affected compared to that of untreated controls (Fig. 5A). Figure 5B and C shows the time course and summary of the effects of verapamil on volume-activated chloride currents, indicating that administration of verapamil had no significant effect on the VACC.

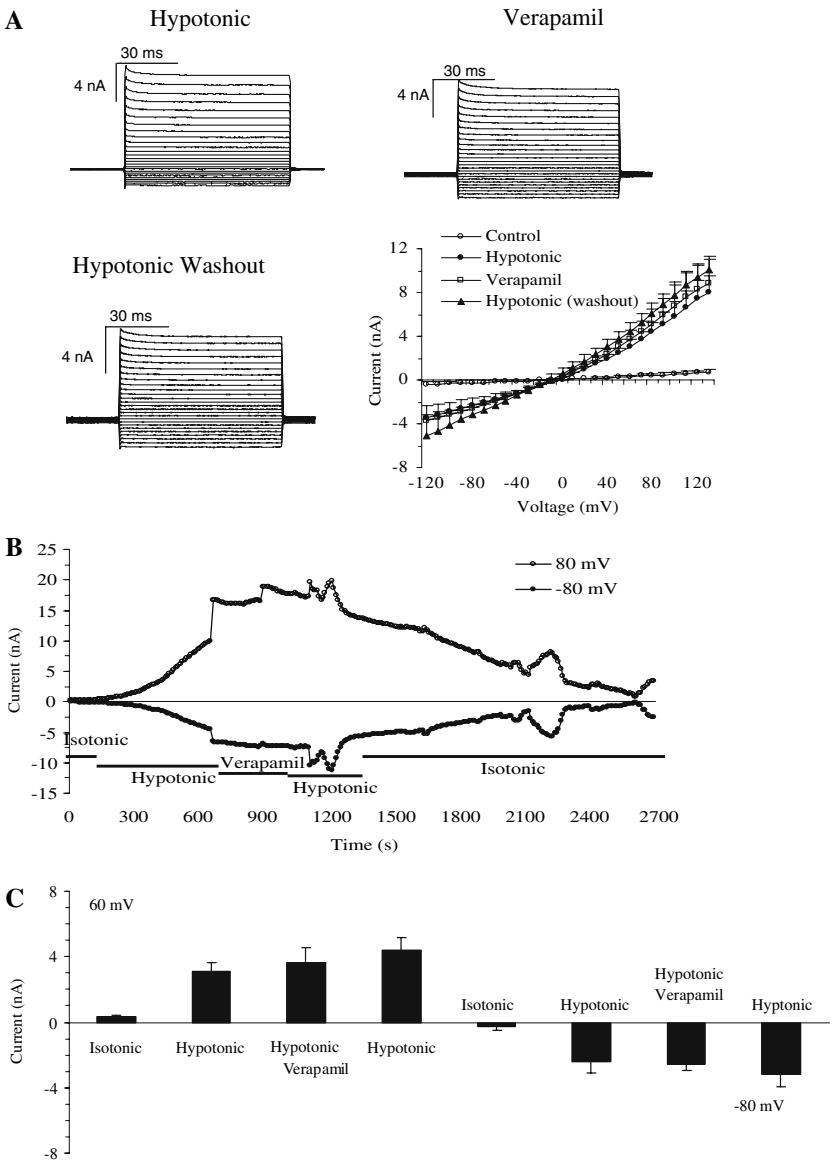

Fig. 5 Effect of verapamil on volume-activated chloride currents. (*A*) Representative traces and *I-V* curve. Currents were measured using voltage steps from –120 to 130 m*V* in 10-m*V* increments at 200 ms, 1 Hz from holding potential 0 m*V*. (*B*) Time course of volume-activated chloride currents and effect of verapamil 20 μM, holding potential 0 m*V*, and voltage step 80 and –80 m*V* at 200 ms, 1 Hz. (*C*) Summary of the effect of verapamil 20 μM on volume-activated chloride currents, $n = 6$, mean ± SD

Calcium-Activated Chloride Currents in MBDCs

To further study the effect of calcium on chloride currents in MBDCs, we examined the effect of ionomycin on chloride currents in isotonic solution. Figure 6A shows representative traces and *I-V* curves of ionomycin-induced calcium-activated chloride currents. An outward current was observed when the cells were perfused with isotonic solution containing ionomycin (1 μM), but the currents returned to basal level when ionomycin was washed off ($P < 0.01$ *vs.* ionomycin, $P > 0.05$ *vs.* control). Figure 6B shows a representative time course of ionomycin-induced currents in MBDCs, and Figure 6C shows a summary of the ionomycin-induced calcium-activated chloride currents in MBDCs. The currents were significantly ($P < 0.05$ *vs.* control) stimulated by administration of ionomycin but promptly returned to basal level when ionomycin was washed off ($P < 0.05$ *vs.* ionomycin, $P > 0.05$ *vs.* control).

To further characterize the ionomycin (1 μM)-induced chloride channels, the effect of removing extracellular calcium on the ionomycin-induced chloride current was examined. As shown in Figure 7A, ionomycin had no significant effect on basal chloride current without extracellular calcium in the bathing solution. When the cholangiocytes were exposed to the solution containing NPPB (40 μM) and ionomycin (Fig. 7B), no significant increase in the chloride current was observed. Figure 7C shows a summary of ionomycin (1 μM)-induced outward chloride current of MBDCs in hypotonic solution containing calcium and that administration of ionomycin further augmented volume-activated chloride currents during hypotonic challenge, suggesting that VACCs and calcium-

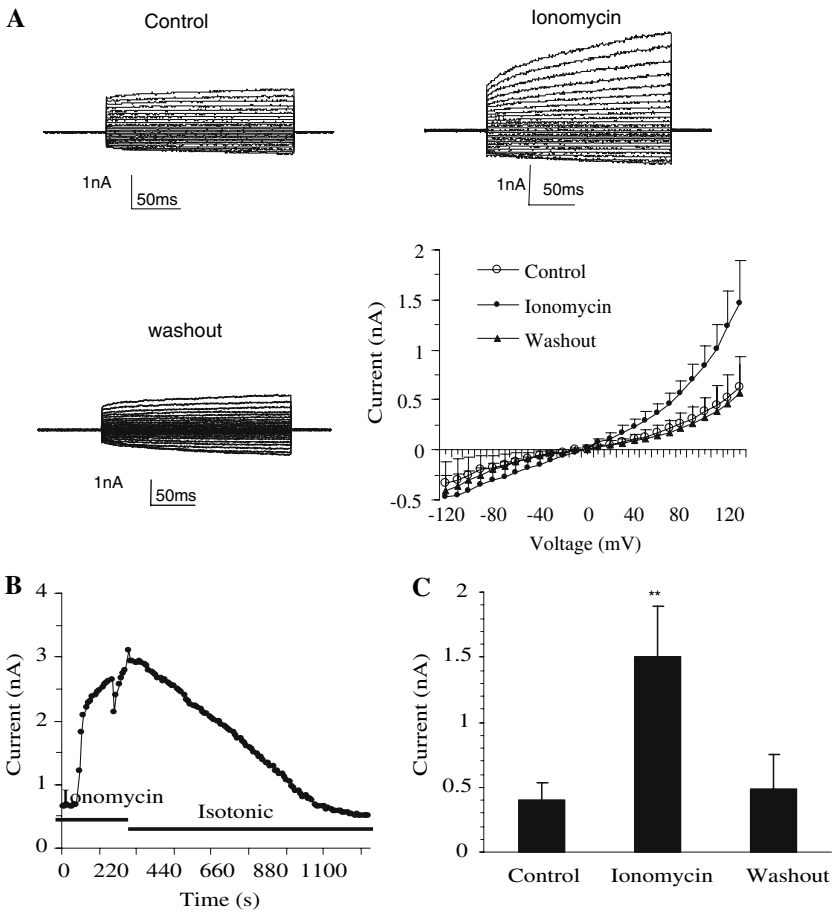

Fig. 6 Calcium-activated chloride current in mouse cholangiocyte line. (A) Representative traces and *I-V* curve. Currents were measured using voltage steps from –120 to 130 m*V* in 10-m*V* increments at 200 ms, 1 Hz from holding potential 0 m*V*, and voltage step 60 and –80 m*V* at 200 ms, 1 Hz. (*B*) Summary of ionomycin-induced chloride currents. (*C*) Summary of the effect of BAPTA-AM on volume-activated chloride currents, n = 5–6, mean ± SD, $^{**}P < 0.01$

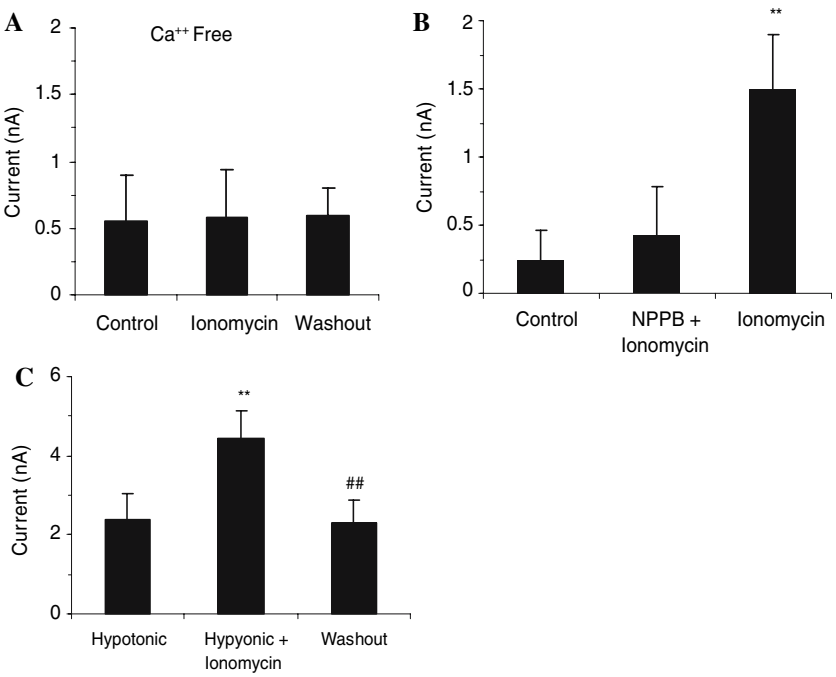

Fig. 7 Effect of ionomycin and BAPTA-AM on volume-activated chloride currents in a mouse cholangiocyte line. (*A*) Summary of the effect of calcium-free hypotonic solution on ionomycin-induced chloride currents. (B) Summary of the blocking effect of NPPB 40 μM on ionomycin-induced chloride currents. (*C*) Summary of ionomycin-induced chloride currents in hypotonic solution, n = 5–6, mean ± SD, $^{\#\#}P$ and $^{**}P < 0.01$

Table 1 Comparison of volume-activated chloride currents and Ca^{2+}-activated chloride currents in mouse cholangiocytes

	Volume-activated chloride currents	Ca^{2+}-activated chloride currents
Functions	Transepithelial transport, pH regulation of intracellular organelles, regulation of excitability and volume regulation (Nilius and Droogmans 2003)	Transepithelial transport and fluid secretion, excitability of neurons and muscle cells and oocyte fertilization (Eggermont 2004)
Molecular identity	Unresolved	Unresolved
Outward rectification	Yes	Yes
Time-dependent activation by high-potential depolarization	No	Yes
Time-dependent inactivation by high-potential depolarization	Yes	No
Extracellular Ca^{2+} dependence	No	Yes
Intracellular Ca^{2+} dependence	No	Yes
Activation by cellular hypotonicity	Yes	No
Inhibitors	NPPB, DIDS, tamoxifen	NPPB, DIDS, niflumic acid

activated chloride channels may be different chloride channels. The ionomycin-induced calcium-activated chloride channels had different electrophysiological characteristics as well as sensitivities to typical channel blockers from VACCs, and these results are summarized in Table 1.

Discussion

As shown previously, the MBDCs used for the present study exhibited a typical VACC, which was inhibited by NPPB and tamoxifen (Chen et al. 2004). The MBDC line is conditionally immortalized by SV40, which expresses cytokeratin 19 and the cystic fibrosis transmembrane conductance regulator (CFTR), confirming its biliary origin, and forms duct-like structures when grown in high density (Paradis et al. 1995). A previous electron microscopic study indicates that these cells are well differentiated and polarized cholangiocytes (Paradis et al. 1995). Therefore, apart from their ability to proliferate at a permissive temperature, MBDCs exhibit normal, differentiated phenotypes of bile duct epithelial cells.

The present study presents the first detailed electrophysiological characterization of the role of intracellular and extracellular calcium in the activation and regulation of VACC in mouse cholangiocytes. Recently, we have shown that mouse cholangiocytes have a VACC which is dependent on chloride concentration (Chen et al. 2004), as previously reported in other cell types (Banderali and Roy 1992; Hazama and Okada 1988; Schmid, Blum and Krause 1998) including the Mz-ChA-1 cholangiocarcinoma cell line (Roman et al. 1996). The currents in MBDCs are low in isotonic conditions but activated by exposure to hypotonic solution, and these volume-activated currents show outward rectification with a varying degree of time-dependent inactivation at depolarizing potentials during hypotonic challenge, as described in other cells (Lewis, Ross and Cahalan 1993; Nilius and Droogmans 2003).

Our whole-cell patch-clamping study indicates that the VACCs of MBDCs are not affected by extracellular or intracellular calcium levels or by calcium channel blockers as reported in the literature (Fatherazi et al. 1994; Best et al. 1996; Wu et al. 1996; Leaney et al. 1997; Pedersen et al. 1998; Von Weikersthal et al. 1999). When exposed to hypotonic solution containing BAPTA-AM or calcium-free hypotonic solution, MBDCs exhibited outwardly rectified VACC currents with time-dependent inactivation, which had the same characteristics and activities as those seen in untreated controls or with normal calcium-containing hypotonic solution (Figs. 2 and 3). These results are consistent with other published results in certain cell types that alterations of extracellular and intracellular calcium did not change the characteristics of VACC current (Fatherazi et al. 1994; Best et al. 1996; Wu et al. 1996; Leaney et al. 1997; Pedersen et al. 1998; Von Weikersthal et al. 1999; Al-Nakkash et al. 2004). Others also reported, as in SV40-immortalized rabbit corneal epithelial cells, that VACC was insensitive to verapamil or removal of extracellular calcium (Al-Nakkash et al. 2004). On the other hand, increases in $[Ca^{2+}]_i$ in other cells, such as human nonpigmented ciliary epithelial cells (Civan, Coca-Prados and Peterson-Yantomo 1994), have been shown to enhance

RVD and calcium pathways to play an important role in cell volume regulation (Montrose-Rafizadeh and Guggino 1991; McCarty & O'Neil, 1991). In some other cells, such as cerebellar astrocytes (Morales-Mulia et al. 1998), RVD and changes in $[Ca^{2+}]_i$ are not related; thus, $[Ca^{2+}]_i$ is thought to be irrelevant as a transduction signal for RVD.

The effect of calcium channel blockers on VACC was also studied to confirm the results seen with removal and chelation of extracellular calcium. Our data did not show any significant effect of calcium channel blocker on VACC as shown in other cell types (Pavenstadt et al. 1996; Viana et al. 1995; Al-Nakkash et al. 2004). However, one study in human fibroblasts reported that nimodipine could inhibit the VACC currents, although its effect was not dependent on extracellular calcium concentration and another dihydropyridine calcium channel blocker had a minor effect on VACC (Chung and Kim 2002). Thus, it is not clear whether those calcium channel blockers had any specific effect on VACC currents by blocking calcium influx.

BAPTA-AM had no significant effect on VACC, while it significantly inhibited the RVD observed with cell volume study. Electrophysiological study indicated that VACC in cholangiocytes is not dependent on calcium for its activation or function; thus, the most likely reason for the inhibitory effect of BAPTA-AM on RVD is the fact that the potassium conductive pathway or another essential component involved in RVD is inhibited by the chelation of intracellular calcium by BAPTA-AM. We also have some evidence that intracellular calcium levels of mouse cholangiocytes do not change during RVD and calcium agonists or calcium channel inhibitors have no effect on RVD in mouse cholangiocytes (*data not shown*). Thus, as in some other cell types (Szucs et al. 1996), calcium may have a permissive role on volume-activated potassium conductances or other cellular processes critical for RVD in cholangiocytes without affecting VACC, as shown in the present study. Consistent with our cell volume study, a previous study in Mz-ChA-1 human cholangiocarcinoma cells also showed that chelation of cytosolic Ca^{2+} by BAPTA-AM inhibited RVD. However, BAPTA-AM also decreased swelling-induced chloride and potassium isotope effluxes (Roman et al. 1996). Although the reason for the apparently different results between the two studies is not clear, the different cells or techniques used may be the cause. Unlike our patch-clamping studies in normal but conditionally immortalized mouse cholangiocyte cells, Roman et al. used an isotope efflux technique, which is not specific for VACC, and human cholangiocarcinoma cells, which may not represent normal physiology.

Furthermore, we have shown that MBDCs also have a calcium-activated chloride channel, which can be activated by ionomycin and blocked by classic chloride channel blockers such as NPPB. Such a calcium-activated chloride channel has been characterized in various epithelial cells, such as human nasal epithelial cells (Jeulin, Guadagnini and Marano 2005), chicken corneal epithelial cells (Connon et al. 2005), rat brain cells (Jeong et al. 2005), human Mz-ChA-1 cholangiocarcinoma cells (Schlenker and Fitz 1996) and rat bile duct epithelial cells (Fitz et al. 1993). A previous patch-clamping study in human Mz-ChA-1 cholangiocarcinoma cells showed that ionomycin activated calcium-activated chloride channels in the cell-attached configuration (Schlenker and Fitz 1996). The calcium-activated Cl^- currents showed outward rectification, time-dependent activation at depolarizing potentials and reversal near the equilibrium potential for Cl^-. The ionomycin-induced Cl^- currents were inhibited by the Cl^- channel blocker DIDS in rat bile duct epithelial cells. The calcium-activated chloride channels are different from VACCs and have somewhat different properties as well (Table 1). The present results are consistent with the data on calcium-activated chloride currents reported in the literature and indicate that separate calcium-activated chloride channels exist in mouse bile duct epithelial cells, which participate in fluid and electrolyte secretion in intrahepatic bile duct epithelial cells (Eggermont 2004). Previously, we have shown that cholangiocytes from cystic fibrosis mouse livers have an impaired RVD, which is thought to be from impaired volume-regulated potassium conductance, rather than chloride conductance (Cho, Siegrist and Zinzow 2004). Thus, VACCs and/or calcium-activated chloride channels are functional in cystic fibrosis cholangiocytes and can likely provide alternative chloride channels for biliary secretion in the absence of a functioning CFTR chloride channel in these cells.

In summary, the present study presents the first detailed data on the role of extracellular and intracellular calcium on VACCs in mouse cholangiocytes. Our results indicate that cholangiocytes have an outwardly rectified VACC, which is activated by hypotonic challenge and inhibited by classical chloride channel inhibitors such as NPPB and tamoxifen but is not affected by the removal and chelation of extracellular or intracellular calcium or calcium channel blocker. Considering various vital functions of the VACC and calcium in cholangiocytes in cell volume regulation, bile secretion, pH regulation, etc., the present study provides an important understanding that the VACC in cholangiocytes is not directly regulated by calcium. Nevertheless, we provide cell volume data indicating that intracellular calcium plays an important role in RVD of cholangiocytes. Since the present patch-clamping study did not show any significant effect of calcium on VACC, this observed inhibitory effect of chelating intracellular calcium on RVD is likely due to its effect on potassium conductive pathways or another essential component involved in RVD. Considering the vital roles of cell volume regulation,

further study of signal transduction pathway(s) involved in cell volume regulation and in the activation of VACCs in normal and diseased cholangiocytes should provide important insight into the pathological processes implicated in various cholangiopathies.

Acknowledgement W. K. C. was supported by an Indiana University Biomedical Research grant. National Institute of Diabetes and Digestive and Kidney Diseases Grants K08-DK-02613 and R03-DK-61409. And a Cystic Fibrosis Research Grant from Cystic Fibrosis Foundation. We appreciate the technical help of Guangqin Zhang in maintaining cell cultures.

References

Al-Nakkash L, Iserovich P, Coca-Prados M, Yang H, Reinach PS (2004) Functional and molecular characterization of a volume-activated chloride channel in rabbit corneal epithelial cells. J Membr Biol 201:41–49

Banderali U, Roy G (1992) Activation of K^+ and Cl^- channels in MDCK cells during volume regulation in hypotonic media. J Membr Biol 126:219–234

Basavappa S, Chartouni V, Kirk K, Prpic V, Ellory JC, Mangel AW (1995) Swelling-induced chloride currents in neuroblastoma cells are calicum dependent. J Neurosci 15:3662–3666

Best L, Sheader EA, Brown PD (1996) A volume-activated anion conductance in insulin-secreting cells. Pfluegers Arch 431:363–370

Chen BY, Nicol G, Cho WK (2004) Electrophysiological characterization of volume-activated chloride currents in mouse cholangiocyte cell line. Am J Physiol 287:G1158–G1167

Cho WK (2002) Characterization of regulatory volume decrease in freshly isolated mouse cholangiocytes. Am J Physiol 283:G1320–G1327

Cho WK, Siegrist VJ, Zinzow W (2004) Impaired regulatory volume decrease in freshly isolated cholangiocytes from cystic fibrosis mice: Implications for cystic fibrosis transmembrane conductance regulator effect on potassium conductance. J Biol Chem 279:14610–14618

Chung MK, Kim HCH (2002) Volume activated chloride currents from human fibroblasts: Blockade by nimodipine. Gen Physiol Biophys 21:85–101

Civan MM, Coca-Prados M, Peterson-Yantorno K (1994) Pathways signaling the regulatory volume decrease of cultured nonpigmented ciliary epithelial cells. Invest Ophthalmol Vis Sci 35:2876–2886

Connon CJ, Kawasaki S, Liles M, Koizumi N, Yamasaki K, Nakamura T, Quantock AJ, Kinoshita S (2006) Gene expression and immunolocalisation of a calcium-activated chloride channel during the stratification of cultivated and developing corneal epithelium. Cell Tissue Res 323:177–182

Diaz M, Valverde MA, Higgins CF, Rucareanu C, Sepulveda FV (1993) Volume-activated chloride channels in Hela cells are blocked by verapamil and dideoxyforskolin. Pfluegers Arch 422:347–352

Eggermont J (2004) Calcium-activated chloride channels: (Un)known, (un)loved? Proc Am Thorac Soc 1:22–27

Fatherazi S, Izutsu KT, Wellner RB, Belton CM (1994) Hypotonically activated chloride current in HSG cells. J Membr Biol 142:181–193

Fitz JG, Basavappa S, McGill J, Melhus O, Cohn JA (1993) Regulation of membrane chloride currents in rat bile duct epithelial cells. J Clin Invest 91:319–328

Graf J, Haussinger D (1996) Ion transport in hepatocytes: Mechanisms and correlations to cell volume, hormone actions and metabolism. J Hepatol 24:53–77

Hazama A, Okada Y (1988) Ca^{2+} sensitivity of volume-regulatory K^+ and Cl^- channels in cultured human epithelial cells. J Physiol 402:687–702

Hoffmann EK, Simonsen LO (1989) Membrane mechanisms in volume and pH regulation in vertebrate cells. Physiol Rev 69:315–382

Jeong SM, Park HK, Yoon IS, Lee JH, Kim JH, Jang CG, Lee CJ, Nah SY (2005) Cloning and expression of Ca^{2+}-activated chloride channel from rat brain. Biochem Biophys Res Commun 334:569–576

Jeulin C, Guadagnini R, Marano F (2005) Oxidant stress stimulates Ca^{2+}-activated chloride channels in the apical activated membrane of cultured nonciliated human nasal epithelial cells. Am J Physiol 289:L636–L646

Kirk K (1997) Swelling-activated organic osmolyte channels. J Membr Biol 158:1–16

Lang F, Busch GL, Ritter M, Volkl H, Waldegger S, Gulbins E, Haussinger D (1998) Functional significance of cell volume regulatory mechanisms. Physiol Rev 78:247–306

Leaney JL, March SJ, Brown DA (1997) A swelling-activated chloride current in rat sympathetic neurons. J Physiol 501:555–564

Lemonnier L, Vitko Y, Shuba YM, Vanden Abeele F, Prevarskaya N, Skryma R (2002) Direct modulation of volume-regulated anion channels by Ca^{2+} chelating agents. FEBS Lett 521:152–156

Lewis RS, Ross PE, Cahalan MD (1993) Chloride channels activated by osmotic stress in T lymphocytes. J Gen Physiol 101:801–826

Li GR, Yang BF, Sun HY, Baumgarten CM (2000) Existence of a transient outward K current in guinea pig cardiac myocytes. Am J Physiol 279:H130–H138

Lira M, Schteingart CD, Steinbach JH, Lambert K, McRoberts JA, Hofmann AF (1992) Sugar absorption by the biliary ductular epithelium of the rat: Evidence for two transport systems. Gastroenterology 102:563–571

McCarty NA, O'Neil RG (1991) Calcium-dependent control of volume regulation in renal proximal tubule cells: I. Swelling-activated Ca^{2+} entry and release. J Membr Biol 123:149–160

Montrose-Rafizadeh C, Guggino WB (1991) Role of intracellular calcium in volume regulation by rabbit medullary thick ascending limb cells. Am J Physiol 260:F402–F409

Morales-Mulia S, Vaca L, Hernandez-Cruz A, Pasantes-Morales H (1998) Osmotic swelling-induced changes in cytosolic calcium do not affect regulatory volume decrease in rat cultured suspended cerebellar astrocytes. J Neurochem 71:2330–2338

Nilius B, Droogmans G (2003) Amazing chloride channels: An overview. Acta Physiol Scand 177:119–147

Nilius B, Eggermont J, Voets T, Buyse G, Manolopoulos V, Droogmans G (1997) Properties of volume-regulated anion channels in mammalian cells. Prog Biophys Mol Biol 68:69–119

Paradis K, Le ON, Russo P, St-Cyr M, Fournier H, Bu D (1995) Characterization and response to interleukin 1 and tumor necrosis factor of immortalized murine biliary epithelial cells. Gastroenterology 109:1308–1315

Pavenstadt H, Huber M, Fischer KG, Gloy J, Leipziger J, Schollmeyer P, Greger R (1996) Swelling of rat mesangial cells induces a Ca^{2+}-dependent Cl^- conductance. Pfluegers Arch 431:706–712

Pedersen SF, Prenen J, Droogman G, Hoffmann EK, Nilius B (1998) Separate swelling- and Ca^{2+}-activated anion currents in Ehrlich ascites tumor cells. J Membr Biol 163:97–110

Roman RM, Wang Y, Fitz JG (1996) Regulation of cell volume in a human biliary cell line: Activation of K^+ and Cl^- currents. Am J Physiol 271:G239–G248

Sardini A, Amey JS, Weylandt KH, Nobles M, Valverde MA, Higgins CF (2003) Cell volume regulation and swelling-activated chloride channels. Biochim Biophys Acta 1618:153–162

Schlenker T, Fitz JG (1996) Ca^{2+}-activated $C1^{-}$ channels in a human biliary cell line: Regulation by Ca^{2+}/calmodulin-dependent protein kinase. Am J Physiol 271:G304–G310

Schmid A, Blum R, Krause E (1998) Characterization of cell volume-sensitive chloride currents in freshly prepared and cultured pancreatic acinar cells from early postnatal rats. J Physiol 513:453–465

Singh AK, Venglarik CJ, Bridges RJ (1995) Development of chloride channel modulators. Kidney Int 48:985–993

Szucs G, Heinke S, Droogmans G, Nilius B (1996) Activation of the volume-sensitive chloride current in vascular endothelial cells requires a permissive intracellular Ca^{2+} concentration. Pfluegers Arch 29:336–343

Viana F, Van Acker K, De Greef C, Eggermont J, Raeymaekers L, Droogmans G, Nilius B (1995) Drug-transport and volume-activated chloride channel functions in human erythroleukemia cells: Relation to expression level of P-glycoprotein. J Membr Biol 145:87–98

Von Weikersthal SF, Barrand MA, Hladky SB (1999) Functional and molecules characterization of a volume-sensitive chloride current in rat endothelial cells. J Physiol 516(pt 1):75–84

Wu J, Zhang JJ, Poppel H, Jacob TJ (1996) P-protein regulates a volume-activated chloride current in bovine non-pigmented ciliary epithelial cells. J Physiol 491(pt 3):743–755